Supplementary information for: Blockley et al. "The resilience of postglacial hunter-gatherers to abrupt climate change"

1. Background to the site

a) Summary of excavations at Star Carr and around Lake Flixton

Star Carr is one of a number of Mesolithic sites that has been recorded around the basin of the Palaeo Lake Flixton. The infilling of the lake has helped to preserve faunal remains and material culture made from wood, bone, and antler as well as evidence for the contemporary environment, making this area one of the most important early prehistoric landscapes in Europe. Star Carr originally lay on the shore of a large peninsula at the western end of the lake. It was first discovered in 1948 by a local amateur archaeologist, John Moore, and was then excavated by Grahame Clark between 1949 and 1951[1]. Clark targeted the waterlogged area on the margins of the lake, recovering a large assemblage of animal bone, organic artefacts and lithic material.

Further work was undertaken in the area from 1976-1985, directed by Tim Schadla-Hall as part of a rescue campaign in advance of the development of a waste disposal plant at Seamer Carr area, on the northwest edge of the basin. This resulted in the discovery of a number of areas of Late Upper Palaeolithic and Mesolithic sites, two of which (Seamer Carr sites C and K) were the subject of large, open area excavation. From 1985, the Vale of Pickering Research Trust undertook extensive surveys of the southern lake shore, conducting auger surveys to map the topography of the basin and identifying further areas of Mesolithic activity through a programme of test-pitting and small scale excavation. Some of these areas underwent further exploration but never on the scale of the Seamer sites[2,3].

At Star Carr, further excavations were undertaken in the 1980s to provide a more precise account of the local environments contemporary with the occupation of the site. To achieve this an 18 m long trench (VP85A) was excavated through the lake edge deposits c. 20 m to the east of the area investigated by Clark. This research not only provided further environmental evidence but also recorded a dense scatter of worked flint, faunal remains and what appeared to be a wooden platform. These unexpected discoveries demonstrated that activity at Star Carr was far more extensive than Clark had realised and that there was considerable potential for further archaeological material in the surrounding deposits. However, what remained unclear was how this new material related to the part of the site investigated by Clark.

This new study is based on more extensive fieldwork from 2004 to 2015, culminating in the excavation of large open areas of both the wetland and dryland parts of the site. Two main phases of archaeological and associated palaeoenvironmental work were undertaken at Star Carr. Phase 1 (2003-2010) sought to characterise the local stratigraphy and the nature, extent, and levels of preservation of the archaeological material in both the wetland and dryland parts of the site. The area around the site was augered in order to map the Star Carr peninsula and the adjacent parts of the lake basin, a series of long narrow trenches were excavated through the sequence of peat deposits at the edge of the lake and two earlier trenches were re-excavated and extended, whilst the Mesolithic dry ground was sampled through fieldwalking, test pitting, and the excavation of a large trench. Phase 2 (2013-2015) consisted of large scale, open area excavation across the former lake shore and the adjacent dryland area incorporating the earlier trenches that had been excavated at the site.

b) the landscape and palaeoenvironmental record of the Vale of Pickering

Palaeolake Flixton was a small lake system that developed after the retreat of glacier ice associated with the Last Glacial Maximum[4,5]. Locally the ice maximum occurred between ~20-17 ka and subsequent eastward retreat of the ice toward the North Sea Basin left a series of outwash gravels with many basins of irregular sized and distributed randomly across the eastern Vale of Pickering. The largest of these basins was Palaeolake Flixton dammed by moraines and outwash gravel highs to the west. Previous work on this lake has focussed on detailing the sediments in the lake and relating them to the archaeological record of surrounding sites. Palynological, radiocarbon and sedimentological evidence suggested that sediments formed within the lake during the Lateglacial and that there was an active lake through into the Early Holocene[4,5,6].

In order to understand the formation of the lake record in more detail and to select the best sample material for high resolution palaeoclimatic and palaeoenvironmental reconstruction, we have undertaken a detailed basin wide auger and survey of the lacustrine sediments to the east of Star Carr and north of Flixton Island (Figure 1 main text). Palmer *et al.*, [7] discovered that the lake bathymetry was more irregular than previously described by Cloutman[8] and which is related to complex proglacial and ice marginal processes during deglaciation. Based on this survey two cores were selected for detailed analyses due to their long early Holocene sediment profiles and proximity to the archaeological sites (cores B and C in main text Figure 1).

2. The results of the new Archaeological investigations

Supplementary Figure 1 The key discoveries found at Star Carr from 2010-2015.

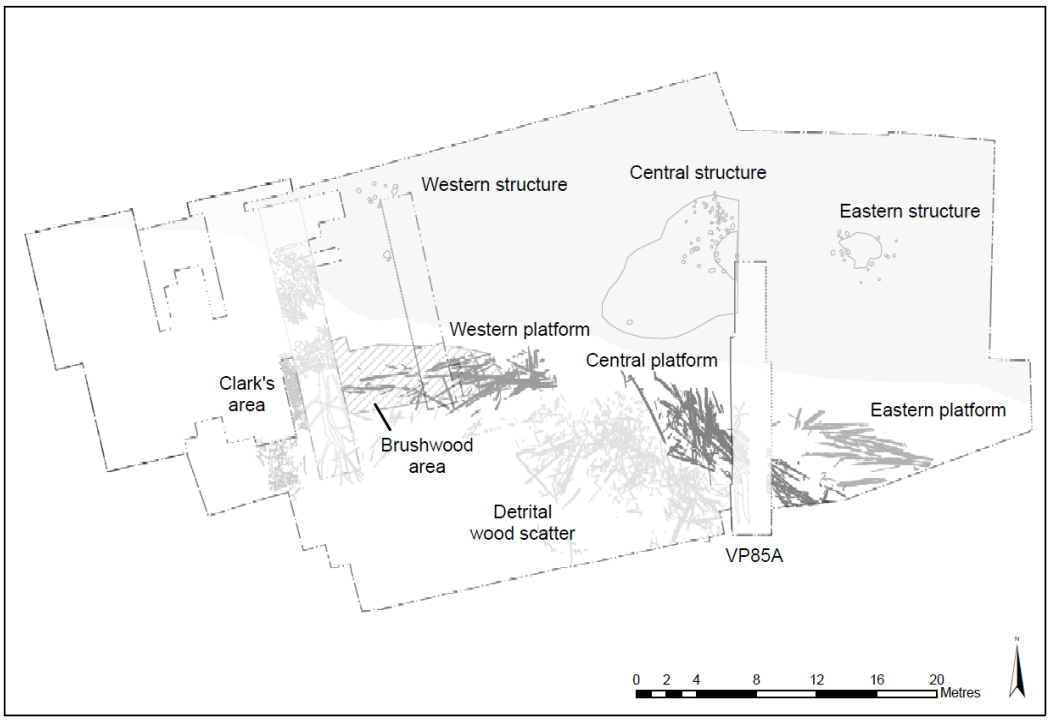

The large scale excavations presented in this study revealed a number of important features across the dryland and lake edge (Supplementary Figure 1). Three structures were found on the dryland: 1. the western structure was defined by a circular area dense in flint debris and a large quantity of burnt flint. In addition a number of ephemeral postholes were discovered. 2. The

central structure was defined by a central hollow, infilled with darker sediment, surrounded by postholes. Further postholes in the area suggest the presence of at least one other structure. 3. The eastern structure was defined by a central hollow, infilled with darker sediment, surrounded by postholes and a large quantity of struck flint within the structure.

A range of different deposits were found in the wetland, discussed from left to right on Supplementary Figure 1. A small area of sediments and artefacts characteristic of those encountered during Clark's excavation remained in situ in one of his baulks (termed Clark's area). This had an extremely high density of finds: flint, faunal remains and organic artefacts including barbed points and antler headdresses/masks.

The western platform was a large wooden structure situated on what would have been the lakeshore (Supplementary Figure 2). The western part of the platform was both under- and overlain by naturally occurring brushwood (having washed in or fallen from trees on the lake shore) within which was evidence of worked wood demonstrating human activity in this area.

The detrital wood scatter consisted of 1329 individual pieces of wood, including roundwood, split and unsplit timbers, and occasionally entire trees, forming a large, roughly linear arrangement 25.8 m long and up to 8.5 m wide (Supplementary Figure 3). The arrangement of the wood lacks any appreciable form or clear phases of deposition or accumulation. However, in terms of its overall shape there is a clear gap amongst the wood on the south-west side of the scatter that coincides with a large concentration of animal bone. The linear form of the scatter, together with the faunal remains deposition, suggest that the wood was deposited to stabilise the soft basal sediments and allow people to access areas of deeper water, possibly (though not necessarily exclusively) for the purposes of depositing animal remains.

Supplementary Figure 2 brushwood (left) western platform (right)

Supplementary Figure 3 The detrital wood scatter.

Both the central and eastern platforms (Supplementary Figure 4) are large wooden structures situated on what would have been the lake shore and are similar in form to the western platform. Other features, artefacts or environmental events which have been dated and which have been included on main text Figure 4 are:

- TPQ fen flint: a relatively dense scatter of worked flint recorded from the upper reed peat and wood peat, which was deposited at the transition to a fen/carr environment (environmental zone 3). The material reflects the expansion of tasks associated with the dry ground onto the more terrestrialised wetlands, and represents the stratigraphically latest phase of occupation on the site
- burning events 1, 2 and 3: three episodes of prolonged burning previously identified[6] on the basis of micro- and macro-charcoal present in pollen profiles recorded from the lake edge deposits.
- SC22 scatter: a scatter of worked flint associated with antler working recorded from the lake edge deposits at the eastern end of the site. The material occupies a similar stratigraphic position to the TPQ fen flint and represents a late episode of activity within the more terrestrialised wetlands.
- bark mat: a mat constructed of bark was found within the peat on the edge of the lake. There was evidence it had been placed there but no evidence of associated activities
- bow: a possible bow was found to the south of Clark's area, part of which was directly dated
- burnt area 318: this is an area of burning within the peat possibly associated with a flint scatter where axes had been made. The context number was 318
- activity in the area of peat over marl: to the southeast of Clark's area was a large mound of naturally occurring marl with peat over it. Evidence of human activity was provided in the form of some faunal remains and modified birch bark rolls

- activity north of Cutting III: this is located north of Clark's area. Here there was evidence of bead manufacture and possible hearths, alongside faunal remains and birch bark rolls
- Birch bark rolls in Clark's area: birch bark rolls were found through the peat sequence in Clark's area

Supplementary Figure 4 Central platform (left); (right) eastern platform top, with part of central platform below it - this was truncated by the VP85A trench excavated in 1985 (see Supplementary Figure 1).

3. Results from the archaeological lake edge macrofossil analysis

The macrofossil profiles (Supplementary Figure 5) have been divided into three environmental/chronological zones on the basis of the changing composition of the assemblages. The profiles all show a similar pattern in terms of the quantities and range of plant macrofossils, and how these change over time and will be discussed together.

Zone-1

Sedimentation began in standing water with emergent vegetation present around the sampling points. Species diversity is relatively high reflecting both the richness of the surrounding wetland vegetation and the wide source area of the profiles. At least two species of *Carex* were present on the basis of nutlet morphology, though only one (*C. paniculata*) could be identified, and a suite of other emergent and aquatic plants were represented by seeds and fruits, and in the case of *Phragmites australis* by stem tissue that formed the coarse component of the sediment. Some species may have been present locally (particular *Phragmites*) though given the dispersive nature of the seeds and fruits of many aquatic and emergent plants the assemblage probably reflects the diversity of the wetlands more widely. Terrestrial plants are best represented by the remains of trees (species of *Betula pubescens*, *Populus (*including *P. tremula),* and to a lesser extent *Salix*), which were growing close enough to the shore for their macrofossils to be transported into the lake. Other terrestrial or fen species are much more poorly represented, probably reflecting the more limited dispersal of their seeds.

Zone-2

The start of the zone sees a sharp fall in the quantity of plant and bryozoan macrofossils from both aquatic and terrestrial species. Given the different habitat preferences of these species this probably reflects a reduction in the source area of the profiles resulting from a decline in the volume of water reaching the lake edge sediments. The sampling points remained at least periodically submerged, though the gradual decline of aquatic material throughout the zone suggest that the volume of water reaching the area continued to fall. Emergent vegetation

(notably *Phragmites australis*) continued to grow locally whilst *Cladium mariscus* became established, probably in response to the shallower environment.

Zone-3

The absence of aquatic material, from the matrix of the peat, and the paucity of aquatic plant macrofossils from the samples marks the transition to a more terrestrialised fen/carr environment that was largely beyond the reach of the lake water. Both the volume and range of the remaining macrofossils is low, probably a result of the much smaller source area of the profiles. Aerial stems and root (species indeterminate) begin to form a large component of the sediment, reflecting the expansion of shrubs or trees onto the peat in response to the more terrestrial environment, whilst a suite of herbaceous plants (including the fen species *Eupatorium cannabinum*) are represented in the macrofossil assemblage.

These zones are shown in main text Figure 4.

Supplementary Figure 5 Raw Macrofossil data from the lake edge monoliths in the Star Carr sequence (Adapted from Taylor et al.[9] , Copyright Cambridge University Press, reprinted with permission).

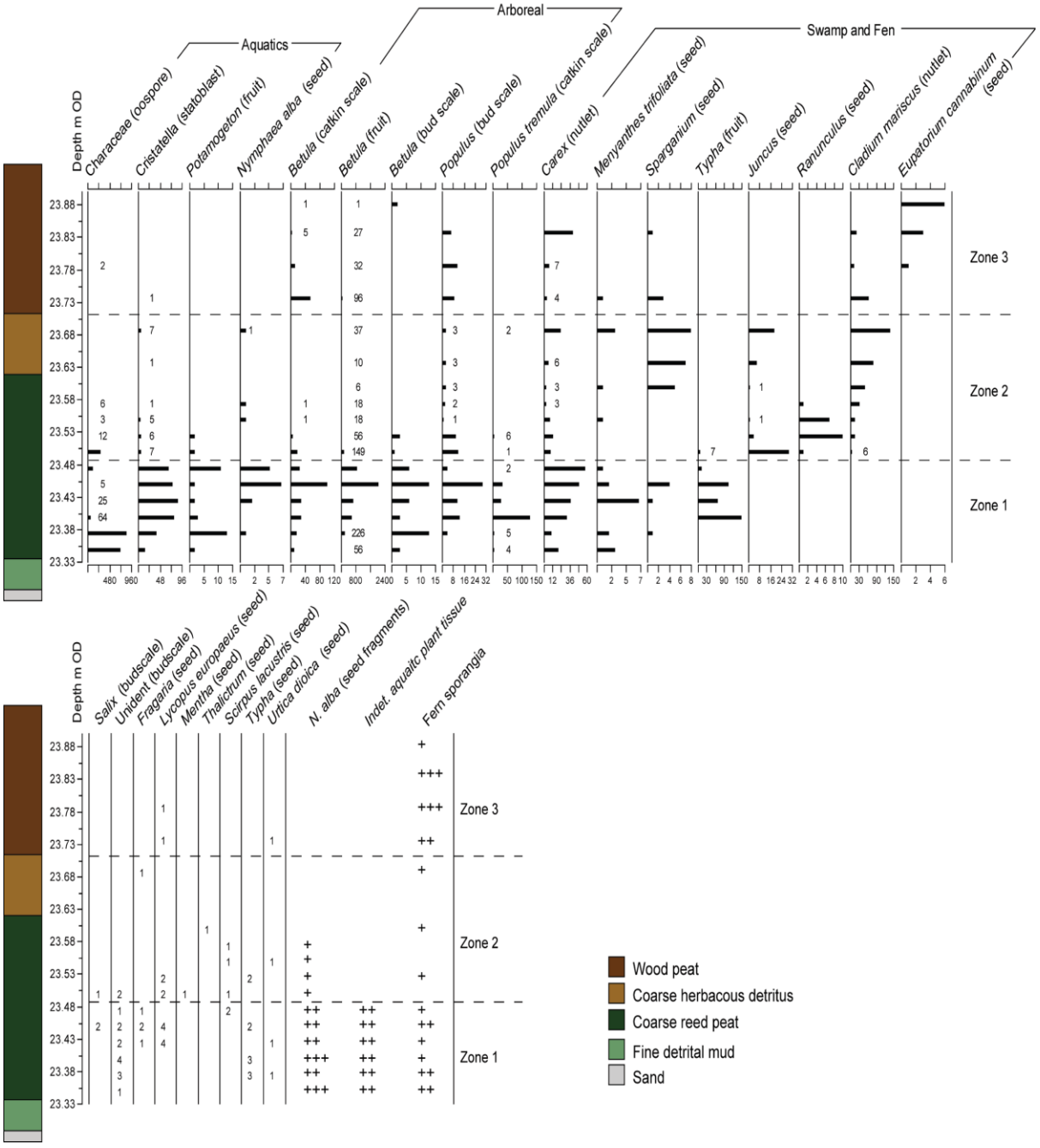

4. Analyses of pollen from the deep lake sediments (cores B and C)

a) Palynology- Star Carr Core B

Within core B, nine statistically significant local pollen assemblage zones (LPAZ; STC B-1:9 Supplementary Figure 6) have been identified and reported as percentages, been rounded to 1 decimal place. Selected pollen data are also shown in main text Figure 6.

STC B-1: 509-465cm: Betula, Pinus, Poaceae, *Artemisia* and *Rumex*

At the base of the zone percentages of Poaceae are high (~48%) accompanied by elevated percentages of *Pinus* and *Artemisia*, 9% and 8% respectively. Progressing towards the top of the zone these taxa decrease in percentages and are replaced by increased percentages of *Betula* (rising from 5% to 34%). Zone 1 is also characterised by high percentages of pre-Quaternary spores (>50% at 501cm).

STC B-2: 465-433cm: Poaceae, Cyperaceae, *Pediastrum*

Zone 2 shows marked decreases of tree taxa from the preceding zone. *Betula* decreases from 34% at the top of the preceding zone to 9% at 445cm. Taxa that are expanding at the expense of *Betula* are predominantly herbaceous taxa with substantial increases in Cyperaceae (up to 20% by 453cm) and Poaceae (up to 44% by 445cm). Perhaps the most significant increase within this zone is the peak in *Pediastrum*. From a zone low of 5% at 461cm *Pediastrum* increases to 38% by 453cm. Other taxa that continue to be present within this zone include: *Artemisia*, *Rumex* and *Thalictrum*. Whilst pre-Quaternary spores are present within this zone they do not exhibit the same percentages as the previous zone.

STC B-3: 433-409cm: Juniperus, Poaceae, Cyperaceae

All tree taxa remain low in percentage during this zone. In contrast to the previous zone, percentages of Poaceae and Cyperaceae have decreased to 21% and 7% respectively by the top of the zone. Equally, the percentages of *Pediastrum* and pre-Quaternary spores have decreased significantly. To account for the reductions in Poaceae and Cyperaceae, *Juniperus* increases markedly to a sequence high of 57% at 429cm.

STC B-4: 409-369cm: Betula, Poaceae, *Juniperus*, *Salix*, *Filipendula*

Zone 4 shows a re-expansion in percentages of *Betula* (from 44% at 405cm to 53% at 373cm). In contrast to the previous zone percentages of *Juniperus* follow a decreasing trend and at 373cm contains <5% TLP. Although observed in previous zones, *Salix* increases to >10% TLP for the first time in the sequence at the mid-point of the zone. This increase is contemporaneous with the first real increase in *Filipendula*. Percentages of Poaeceae and Cyperaceae are similar to the zone beneath. Other taxa that maintain a presence within zone 4 include *Rumex* and the aquatic *Myriophyllum*.

STC B-5: 369-298cm: Betula, Poaceae, *Filipendula*

Whilst percentages of Betula appear quite high, they are lower in value than zone 4 and individual percentages fluctuate between 23-40%. Poaceae, Cyperaceae, *Juniperus* and *Filipendula* are taxa that show similarity with the previous zone. All are stable and continually present and with the exception of Poaceae all <12% TLP.

STC B-6: 298-275cm: Poaceae, Cyperaceae, *Filipendula, Pinus, Rumex, Pediastrum*

A marked change occurs across multiple taxa during this zone. There is a shift to *Pinus* being the dominant tree taxa with percentages of 18% TLP at 289cm. In contrast, *Betula* percentages decrease to a zone low of 15% at 285cm. The two most striking changes within this zone are the rapid increases in Poaceae and *Pediastrum*. Increases of the latter occur first, with increases from 14%, within the previous zone, to 62% at 297cm. Poaceae increases in the subsequent sample, from 17% at 297cm to 46% at 293cm. Both Poaceae and *Pediastum* tail off to lower percentages at the top of the zone. From the base to the middle of the zone *Rumex* increases to 8% TLP. Subsequent changes within this zone include increases in percentages of *Filipendula*. At 293cm *Filipendula* is <1% TLP, however by 281cm it has increased to 19% TLP.

STC B- 7: 275-263cm: Juniperus, Betula, Salix

Zone 7 appears somewhat similar to zone 3 regarding types and trends between taxa. The main taxa within this zone is *Juniperus*, a zone high of 22% occurring at 269cm, with concomitant increases in *Betula*. *Salix* reaches a sequence high during zone 7 of 16% at 273cm. Additional taxa that are present in lower percentages within this zone include Poaceae, *Filipendula* and *Pediastrum*.

STC B-8: 263-215cm: Betula, Pinus, Salix, Dryopteris

The most significant taxa across all spectra within zone 8 is *Betula*. *Betula* demonstrates high percentages (>50%) throughout the whole zone. The other notable tree taxa, despite containing much lower percentages, is *Pinus*. Like *Pinus, Salix* is continually present, between 3% and 10% throughout the zone. Additionally, for the first time in the sequence *Dryopteris* percentages increase (to 8% by 241cm) with associated increases in Filicales.

STC B-9: 215-205cm: Corylus, Betula

The final zone in the sequence is characterised by significant increases in the Coryloid shrubs. From first appearance during the preceding zone, Corylus expands to a zone and sequence high of 68% at 209cm. The only other notable taxa within this zone is *Betula*, however the percentages of *Betula* are reduced to 17% at the 209cm depth.

b) Palynology- Star Carr Core C

From one sample beneath the Vedde Ash in core C up to the end of marl sedimentation in the early Holocene contains 5 statistically significant local pollen assemblage zones (LPAZ; STC C-1:5; Supplementary Figure 7).

STC C-1: 525-343cm: Pediastrum, Cyperaceae, *Betula*, Poaceae, *Pinus*, *Artemisia*

Zone 1 in core C covers over 1.5m of assemblage. It is perhaps most characterised by increasingly elevated percentages of *Pediastrum*. *Pediastrum* shows a slight increasing trend from 27% at 525cm to 44% at 393cm. However, a greater increase is observed between 393-349cm where percentages of *Pediastrum* are sustained at >50%. Coincident with this increase are elevated percentages of Cyperaceae, Poaceae and *Betula*. Whilst percentages are relatively low (<10%) *Artemisia* is continually present.

STC C-2: 343-327cm: Poaceae, *Pinus, Rumex, Potamogeton*

Compared to the previous zone, *Betula* percentages decrease but there is an increase in *Pinus* to 13% by 341cm. Although, the most substantial increases within zone 2 are those of Poaceae; with percentages >35% throughout. Occurring alongside the increases in Poaceae are increases

in *Rumex*. Within zone 1 *Rumex* percentages were generally lower than 5%, however, there is nearly a two-fold increase in percentage to 10% TLP at 329cm. Equally, at 329cm there is a significant spike in *Potamogeton*, from <1% at 333cm to 47% at 329cm. Myriophyllum is also likely to be locally significant during this phase.

STC C-3: 327-315cm: Poaceae, *Filipendula*, *Salix*

Although percentages of Poaceae are reduced at the onset of the zone (26% at 325cm) they increase sharply to 41% by 317cm. Within zone 3 *Filipendula* increases to a sequence maxima of 22% at 325cm before tailing off to lower percentages towards the top of the zone. Other taxa that demonstrate elevated percentages include *Salix* and *Pediastrum*.

STC C-4: 315-303cm: Salix, Juniperus, Betula, Filipendula

Zone 4 is characterised by sequence highs of two taxa, *Salix* and *Juniperus*. Peaks in both taxa occur towards the base of the zone at 313cm and exhibit percentages of 21% and 15% respectively. Percentages of both then show a reducing trend. A similar situation is true for *Filipendula*. Whilst the peak is observed in the previous zone, *Filipendula* shows a reduction from 11% to 7% by 305cm. In contrast to these declining trends, *Betula* shows significant increases within this zone, from 34% at the base to 50% at the zone boundary.

STC C-5: 303-281cm: Betula

The main taxa of any category within zone 5 is Betula. Increasing percentages were observed in zone 4, however within zone 5 all percentages of *Betula* are above 50% with a sequence high of 77% at 281cm. Other notable taxa within this zone include *Pinus*, *Salix*, Poaceae and *Dryopteris*.

Supplementary Figure 6 Core B pollen profiles against depth (redrawn from Milner *et al.*[10])

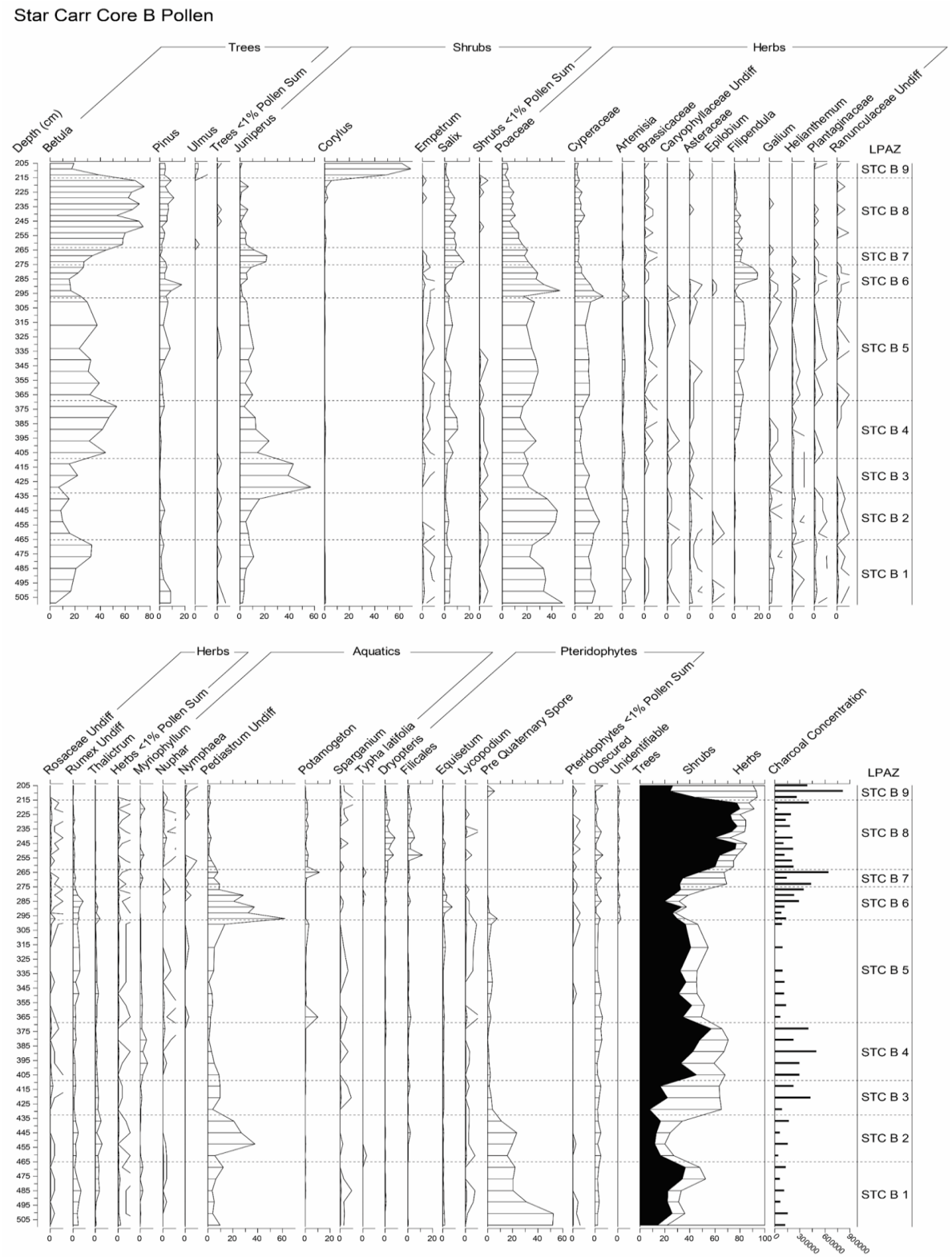

Supplementary Figure 7 Core C pollen profiles against depth (redrawn from Milner *et al.*[10])

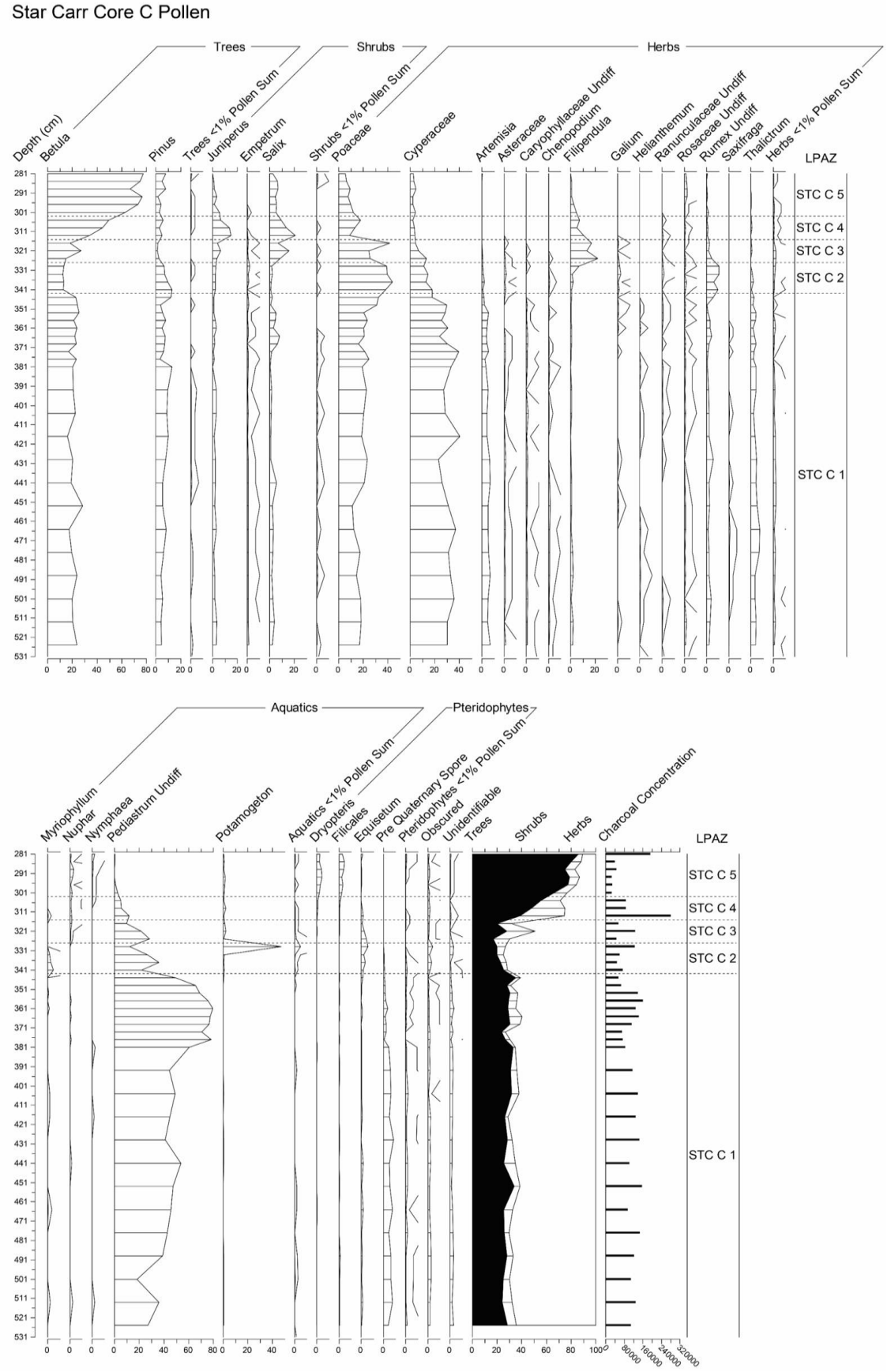

5. Chironomids, CI-T reconstructions and isotopic analyses for Lake Flixton

Supplementary Figure 8 Chironomid Cores B and C showing the full B sequence with the upper c. 15 samples used for the climate model, as the lake record extends into the Pleistocene with some hiatuses, and full core C sequence (all taxa) which we used all for the CI-T in this study.

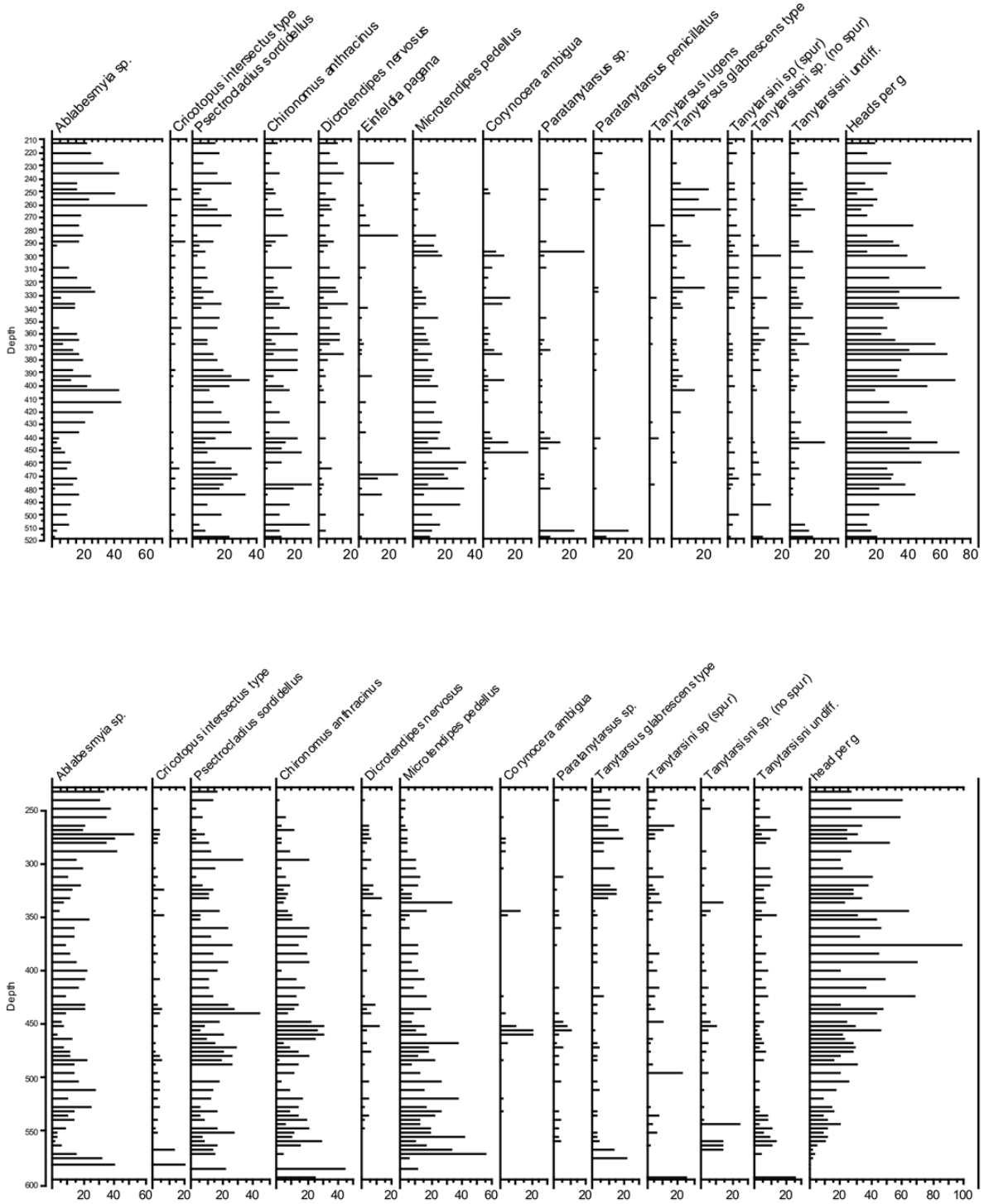

The chironomid sequences (Supplementary Figure 8) are dominated by *Ablabesmyia* and *Paratanytarsus* taxa, both of which typically indicate associations with macrophytes[11], and as such may be indicative of relatively clear and/or shallow waters. There are notable periods where cold adapted taxa occur, such as *Paracladius* in core B, and *Corynocera* in core C, indicative of relatively cool summer temperatures. In order to test the robustness of the CI-T, we undertook some analogue and goodness-of-fit tests on the chironomid data as compared with the Norwegian training set[12]. Goodness-of-fit of the temperature reconstruction was estimated by creating a canonical correspondence analysis (CCA) singly constrained to mean July temperature. Fossil intervals with a squared residual distance value within the most extreme 5 % of values in the Norwegian calibration set were considered to have a poor fit with respect to temperature, those within the most extreme 15 % a 'fair' fit, and those beyond 15 % were considered non-analogue (Supplementary Figure 9). Only 3 data points showed a poor fit, with the rest showing fair to good fits. To determine whether the fossil data had appropriate analogues for mean July temperature reconstructions the data were plotted passively positioned in a PCA of the Norwegian calibration set (Supplementary Figure 10). A robust interpretation is shown by the data transitioning along the temperature gradient[13]. Taxon relative abundances were square-root transformed. All analyses were completed in R version 3.2.2[14] using the rioja, analogue, and vegan libraries.

Supplementary Figure 9: Goodness-of-fit of fossil samples (depth vs. squared residuals).

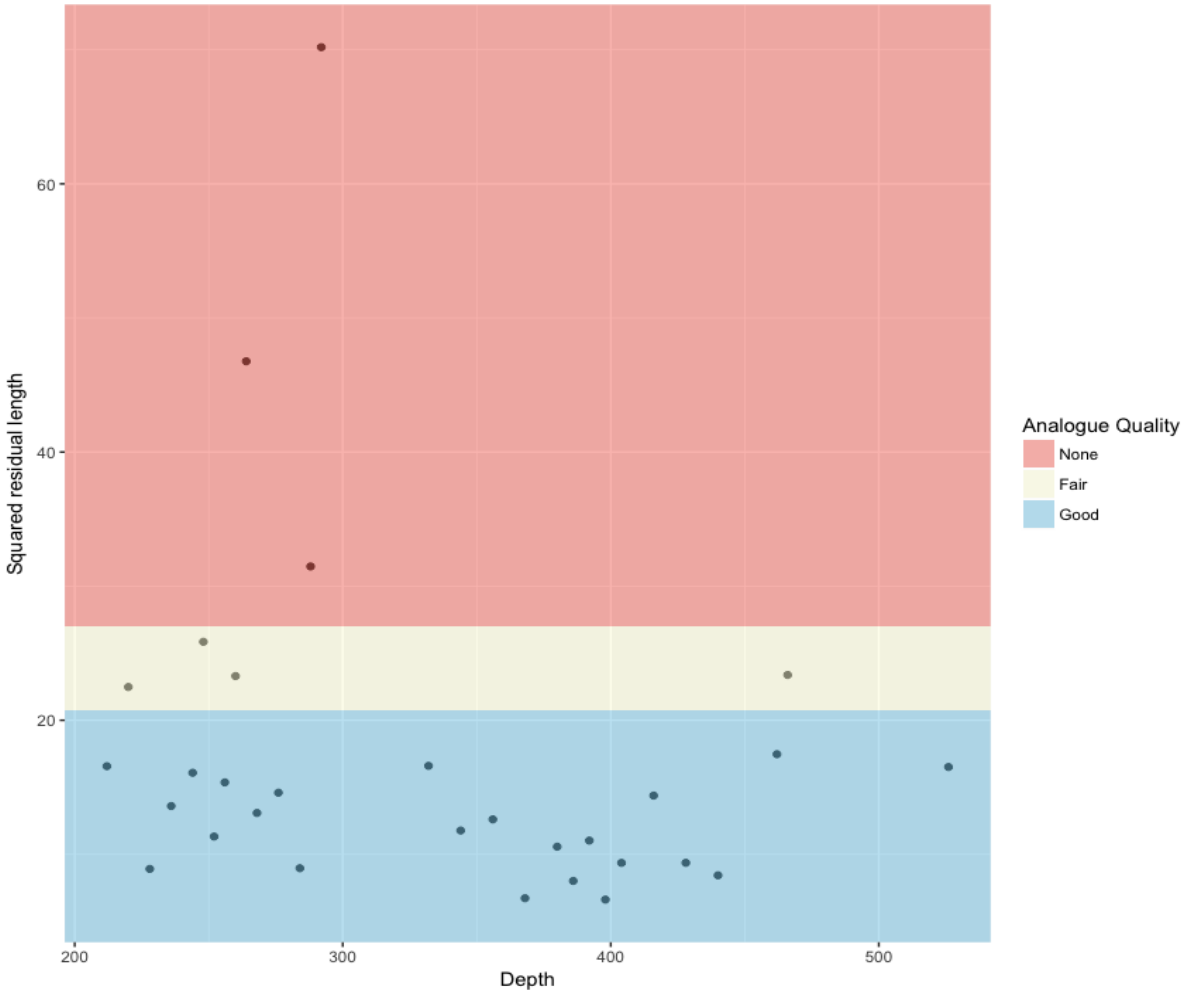

Supplementary Figure 10: Fossil samples (green open circles) passively plotted in a PCA of the Norwegian calibration set[12] . The fossil samples plot mainly along the temperature gradient, suggesting a temperature reconstruction is robust.

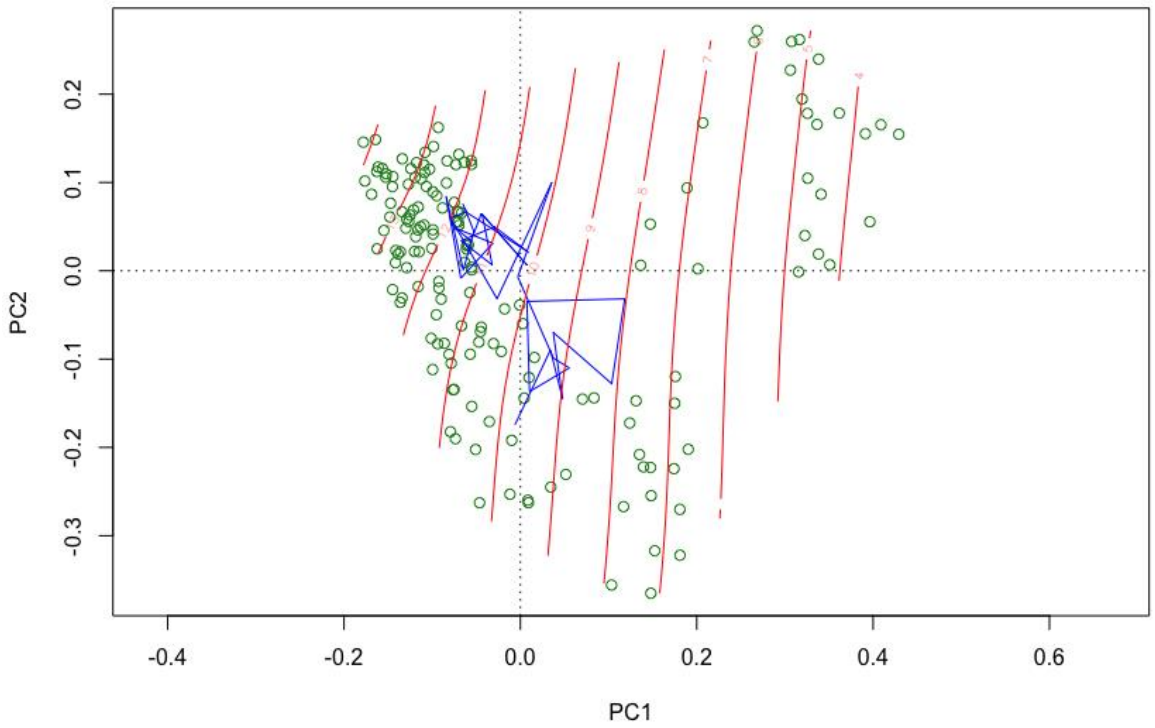

The CI-T $\delta^{18}O$ and $\delta^{13}C$ results from the detailed palaeoclimate study of borehole B from the transect survey are presented in Supplementary Figure 11. This record has marl accumulation from 21.1 m with the early Holocene record in the lower section of 3 m of marl accumulation It is likely that in this core there is a lag between the start of the Holocene and the start of sedimentation, due to the OD height of the core and the time taken for the water table to rise after the Loch Lomond stadial.

Supplementary Figure 11 CI-T and $\delta^{18}O$ and $\delta^{13}C$ from core B against depth in core for the Early Holocene covering ACE 2 and the carbon isotope shift.

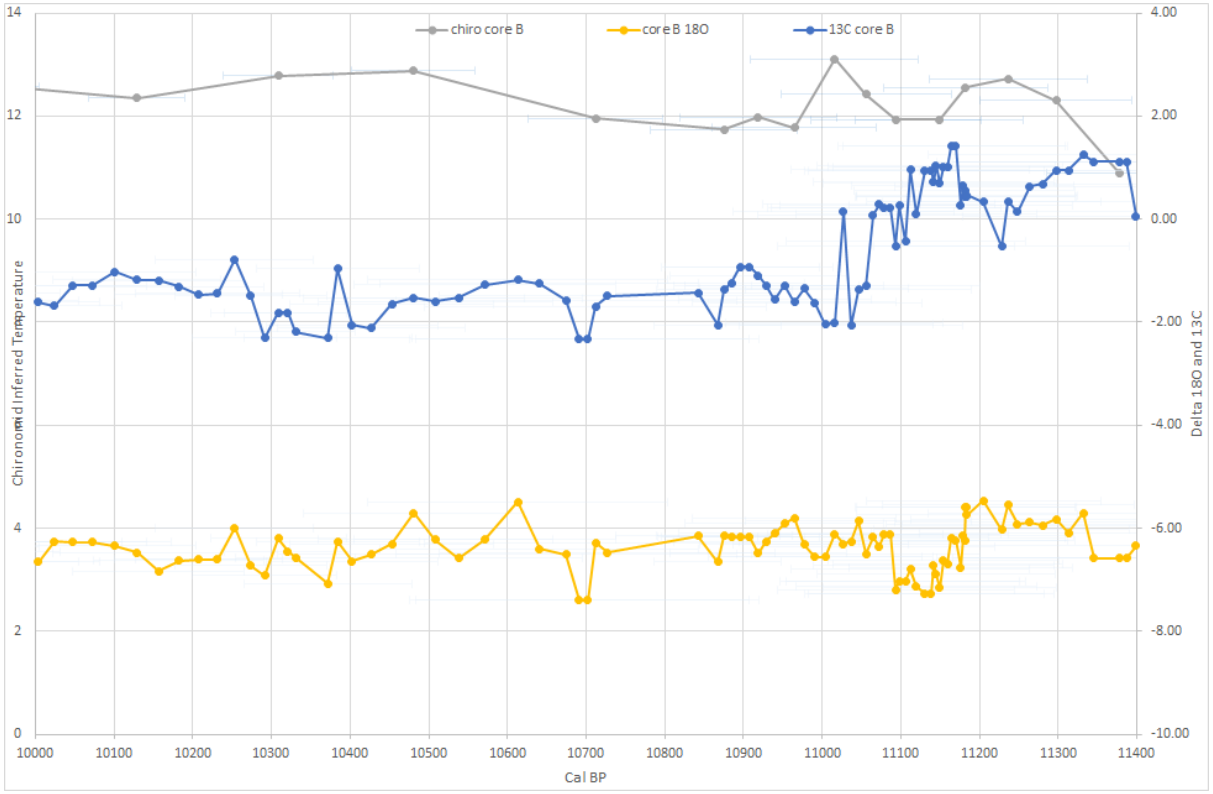

Due to this hiatus, further investigation was undertaken on the transition between clay and marl from 3 m to 5 m in core C (Supplementary Figure 12). This core was known to have a much more extensive record of Loch Lomond stadial sedimentation and is located deeper in the basin, and is thus less likely to have been cut off from sediment supply during periods of low lake level in the Loch Lomond stadial. In addition, this core was known to contain the Vedde Ash tephra, dating to the mid Loch Lomond stadial at a depth of 5.26 m[7], demonstrating sedimentation during the mid Loch Lomond stadial in the form of grey silts and clays that shift to marl formation at 21.5 m OD. As with core B this core was analysed for chironomids and $\delta^{18}O$ and $\delta^{13}C$ and these are detailed in Supplementary Figure 12.

Supplementary Figure 12 CI-T and $\delta^{18}O$ and $\delta^{13}C$ from core C shown against depth from the onset of the Holocene, ACE 1 is centred around 360 cm in the core, note the depleted early Holocene CI-T values, similar to those close to the mid Younger Dryas Vedde Ash.

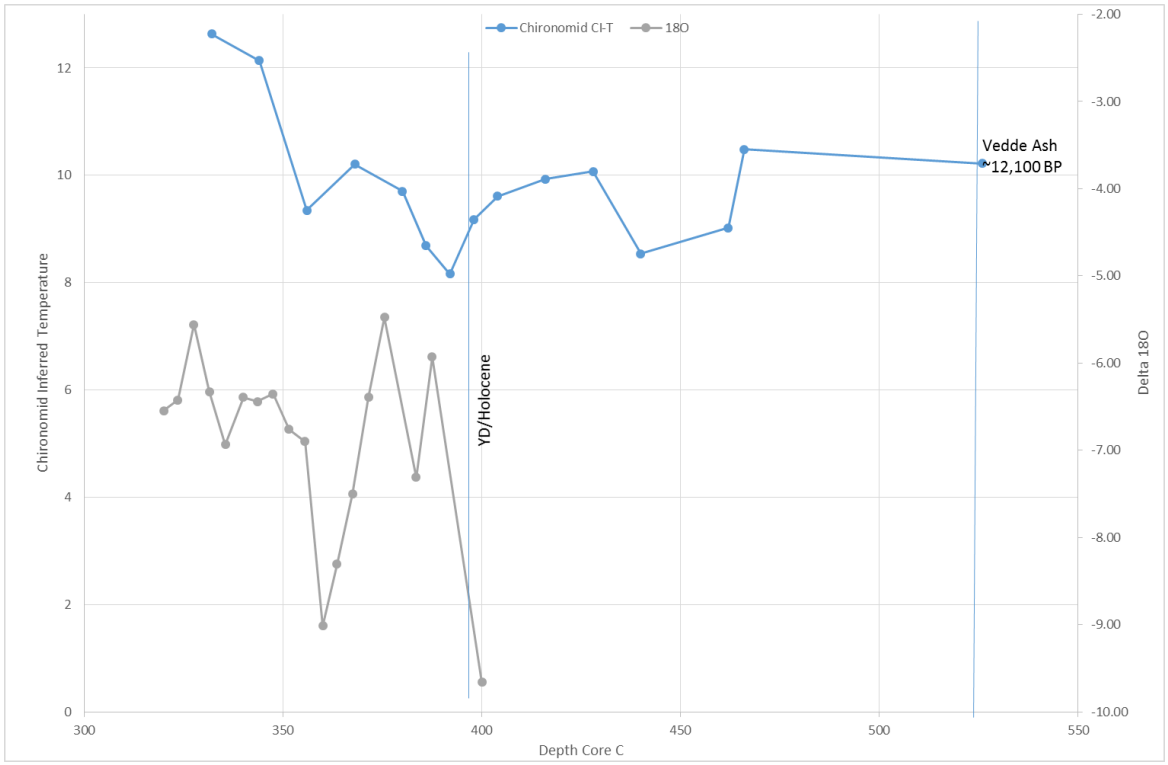

In core C the palaeotemperature proxies show a shift out of Loch Lomond stadial conditions at a depth of 3.87 to 3.85 m below ground surface, with a sharp shift in the oxygen isotopes, but more muted shift in chironomids, suggesting that summer temperatures at the start of the Holocene were still not significantly above the baseline Loch Lomond stadial conditions seen in the values around the time of the Vedde ash at 5.26 m. The Early Holocene continues to be unstable in these cores with fluctuations at 3.75 m and 3.56 m. In core B the CI-T and $\delta^{18}O$ values also indicate a fluctuating Early Holocene climate after the onset of Holocene sedimentation in this core. The $\delta^{18}O$ shows shifts of -2 per mille from initial Holocene warming just after 3 m to the first of several Early Holocene troughs.

6. Tephrochronology

5cm scan sampling of cores C and B for Early Holocene and Younger Dryas age sediments revealed the presence of cryptotephra only in core C. This tephra deposit sits between 540 and 340 cm, but with a main peak of over 2000 shards p/gm at 520-525 cm, tailing down to a few shards per gm by 340cm. The peak of the tephra and the bulk of the deposition sits in grey silty clay sediments interpreted (10) as representing Loch Lomond stadial sediments. In order to determine if more than one tephra was present samples were reanalysed at 1cm resolution and these showed peaks of >1000 shards p/gm at 423 cm but small peaks of 45 shards p/gm at 480

cm and 485 cm. Geochemical analyses of peaks at 523 and 485 cm (Supplementary Table 1) are chemically correlated to the Vedde Ash tephra[7] a widespread tephra found across Europe in the mid Loch Lomond/Younger Dryas stadial and in the Greenland ice cores.

Supplementary Table 1 The major element geochemical data for the Vedde Ash at Star Carr

Label	Ox%(Si)	Ox%(Ti)	Ox%(Al)	Ox%(Fe)	Ox%(Mn)	Ox%(Mg)	Ox%(Ca)	Ox%(Na)	Ox%(K)	Total
SC523_10	70.2	0.2	13.2	3.7	0.1	0.2	1.2	5.5	3.3	98.0
SC523_11	70.8	0.3	13.7	3.8	0.2	0.2	1.3	5.6	3.5	99.8
SC523_12	70.0	0.3	13.3	3.8	0.2	0.2	1.3	5.0	3.4	97.6
SC523_13	71.3	0.4	13.6	3.9	0.1	0.2	1.4	5.1	3.4	99.7
SC523_14	69.7	0.3	13.2	3.5	0.2	0.2	1.3	5.0	3.4	96.9
SC523_15	70.6	0.2	13.2	3.8	0.1	0.2	1.4	5.0	3.5	98.2
SC523_16	69.5	0.3	13.1	3.8	0.1	0.2	1.2	4.9	3.5	96.6
SC523_18	70.4	0.3	13.4	3.7	0.1	0.2	1.3	5.3	3.4	98.4
SC523_19	70.0	0.3	13.0	3.7	0.1	0.2	1.3	5.0	3.5	97.3
SC523_2	70.4	0.3	13.2	3.8	0.2	0.1	1.3	5.4	3.4	98.1
SC523_21	70.9	0.3	13.5	3.5	0.1	0.2	1.4	2.5	3.5	96.5
SC523_22	69.7	0.3	13.1	3.6	0.1	0.2	1.3	5.2	3.5	97.2
SC523_23	70.7	0.3	13.2	3.5	0.1	0.2	1.3	5.5	3.4	98.7
SC523_24	68.9	0.3	13.0	3.8	0.1	0.2	1.3	5.1	3.4	96.6
SC523_25	70.1	0.3	13.3	3.6	0.2	0.2	1.3	5.3	3.5	98.2
SC523_26	70.0	0.4	13.3	3.5	0.1	0.2	1.3	5.1	3.6	98.0
SC523_28	69.5	0.3	13.1	3.5	0.1	0.2	1.4	5.4	3.4	97.0
SC523_29	70.4	0.3	13.4	3.8	0.2	0.2	1.3	5.4	3.4	98.8
SC523_3	69.6	0.3	13.3	3.8	0.2	0.1	1.2	4.9	3.5	97.2
SC523_30	71.0	0.3	13.5	3.8	0.1	0.2	1.4	5.4	3.6	99.4
SC523_31	71.3	0.3	13.7	3.8	0.1	0.2	1.3	5.5	3.5	99.9
SC523_32	70.6	0.5	13.4	3.7	0.2	0.2	1.3	5.3	3.5	99.1
SC523_33	71.3	0.3	13.5	3.4	0.1	0.2	1.3	4.9	3.6	98.8
SC523_4	67.1	0.3	12.8	3.5	0.2	0.2	1.2	5.0	3.3	94.0
SC523_6	70.6	0.3	13.3	3.6	0.2	0.2	1.4	5.3	3.5	98.5
SC523_7	71.8	0.3	13.6	3.6	0.1	0.2	1.3	5.6	3.5	100.4
SC523_9	69.8	0.3	13.2	3.8	0.2	0.1	1.4	5.2	3.5	97.7
SC403_2	69.1	0.3	13.1	3.6	0.1	0.2	1.3	5.0	3.4	96.1
SC403_6	67.8	0.3	13.0	3.5	0.2	0.1	1.3	5.0	3.2	94.7
SC480_3	69.7	0.3	13.1	3.8	0.1	0.2	1.3	5.2	3.4	97.2
SC480_4	69.9	0.3	13.2	3.6	0.2	0.2	1.3	5.4	3.4	97.6
SC480_5	70.6	0.3	13.4	3.4	0.1	0.1	1.4	5.2	3.4	98.2
SC480_8	71.7	0.3	13.3	3.8	0.2	0.2	1.3	3.0	3.5	97.7

7. Chronological Modelling

7a. Lake-edge archaeological and palaeoenvironmental model

Key parameters for different episodes of human activity at Star Carr are illustrated in main text Figure 3, with Highest Posterior Density intervals for these parameters provided in Supplementary Table 2.

Supplementary Table 2 Highest Posterior Density intervals for key parameters of archaeological activities at Star Carr (*OxA-3349* is the start of burning 1, *OxA-33662* is the dated timber from the eastern platform, *SUERC-59177* is the bark mat, and *OxA-25240* is the bow), derived from the model defined exactly by the OxCal CQL2 code files (star_carr_combined_all_v3.oxcal and star_carr_combined_all_v3_additional.oxcal).

Parameter	***Highest Posterior Density interval (cal BP)***	
	(95% probability)	*(68% probability)*
110553	*11695–11675 (1%)* or *11620–11425 (94%)*	*11610–11525 (65%)* or *11475–11460 (3%)*
start Star Carr	*11335–11210*	*11285–11225*
end Star Carr	*10505–10330*	*10475–10390*
OxA-3349	*11020–10895*	*10970–10915*
end of burning 1	*10965–10795*	*10930–10845*
start of burning 2	*10865–10735*	*10830–10765*
end of burning 2	*10755–10580*	*10720–10625*
burning 3	*10685–10485*	*10635–10530*
start wood scatter	*11265–11195*	*11240–11205*
end wood scatter	*11065–10865*	*11045–10950*
start brushwood	*11290–11140*	*11245–11185*
end brushwood	*11040–10870 (12%)* or *10770–10460 (83%)*	*10735–10580*
western platform	*10755–10705*	*10745–10715*
central platform	*10935–10875*	*10920–10890*
OxA-33662	*10895–10710*	*10865–10845 (9%)* or *10830–10745 (59%)*
start Clark area	*11075–11040 (4%)* or *10865–10725 (91%)*	*10800–10750*
end Clark area	*11050–11025 (3%)* or *10780–10660 (92%)*	*10760–10705*
start reed peat in Clark area	*11230–10795*	*11085–10825*
end human in reed peat in Clark area	*10695–10430*	*10660–10520*

start peat over marl	*11145–10805*	*11040–10875*
end peat over marl	*10965–10600*	*10905–10745*
start N of CIII	*11250–10800*	*11200–10975 (66%)* or *10880–10865 (2%)*
end N of CIII	*10760–10435*	*10725–10560*
TPQ fen flint	*10620–10425*	*10555–10465*
SC22 scatter	*10725–10615*	*10705–10655*
burnt area 318	*10915–10770*	*10890–10860 (22%)* or *10855–10795 (46%)*
SUERC-59177	*10750–10655 (94%)* or *10615–10605 (1%)*	*10735–10695*
OxA-25240	*11055–11020 (2%)* or *11010–10955 (6%)* or *10870–10845 (1%)* or *10815–10575 (86%)*	*10770–10650 (62%)* or *10625–10600 (6%)*
start east structure	*11200–10770*	*11130–10970 (57%)* or *10885–10845 (7%)* or *10830–10790 (4%)*
end east structure	*11065–10580*	*11040–10915 (32%)* or *10815–10685 (36%)*
start west structure	*11210–10955 (63%)* or *10935–10745 (32%)*	*11125–10975 (51%)* or *10870–10855 (2%)* or *10830–10765 (15%)*
end west structure	*11060–10575*	*11045–10925 (31%)* or *10790–10685 (37%)*

Key parameters for the establishment of the different environmental zones around the lake edge at Star Carr are illustrated in Supplementary Figure 13, with Highest Posterior Density intervals for these parameters provided in Supplementary Table 3.

Supplementary **Figure 13** Probability distributions for the establishment of the different environmental zones around the lake edge at Star Carr, derived from the model defined exactly by the OxCal CQL2 code files (star_carr_combined_all_v3.oxcal and star_carr_combined_all_v3_additional.oxcal).

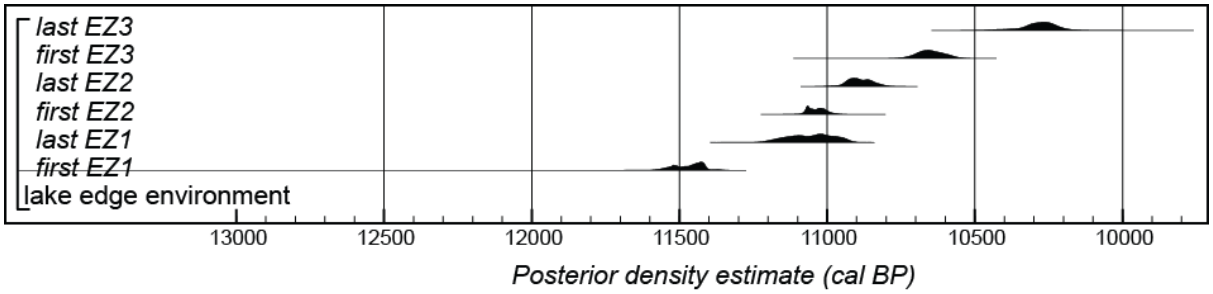

Supplementary Table 3 Highest Posterior Density intervals for the establishment of the different environmental zones around the lake edge at Star Carr, derived from the model defined exactly by the OxCal CQL2 code files (star_carr_combined_all_v3.oxcal and star_carr_combined_all_v3_additional.oxcal).

Parameter	***Highest Posterior Density interval (cal BP)***	
	(95% probability)	*(68% probability)*
Environmental Zones		
first EZ1	*11585–11395 (94%)* or *11385–11360 (1%)*	*11530–11500 (14%)* or *11485–11410 (54%)*
last EZ1	*11195–10920*	*11135–10965*
first EZ2	*11095–10960*	*11075–11005*
last EZ2	*10965–10800*	*10935–10850*
first EZ3	*10745–10555*	*10700–10605*
last EZ3	*10450–10165*	*10330–10215*

The Bayesian model for occupation at Star Carr indicates that human activity on the site began in *11335-11210 cal BP (95% probability; start Star Carr*; main text Figure 3), probably in *11280-11225 cal BP (68% probability)*, by which time a species rich reedswamp environment was present at the lake shore. Occupation during the earliest centuries consisted of repeated episodes of activity, relatively small in scale and focused on specific areas of the site. Archaeologically, the most extensive is the *detrital wood scatter*, a large, broadly linear arrangement of worked wood, animal bone, antler and material culture (including red deer antler headdresses/masks, barbed antler points, and worked flint). The wood was laid down to stabilise the soft basal deposits and formed a trackway from the shore into an area of shallow standing water, probably to facilitate the deposition of the animal bones and artefacts. Woodworking also occurred at an area of the lake shore resulting in the deposition of worked wood into a natural accumulation of brushwood that formed in shallow water at the lake edge (the *brushwood*). Occupation of the dryland also occurred at this time, possibly represented by the use of a post-built circular structure (*central dryland structure (330)*; main text Figure 4), if so this would represent the earliest known structure in the British Isles. This was built in *11290–11175 cal BP (start 330;* probably in *11245–11195 cal BP (68% probable).*

Conditions at the lake edge became shallower and the swamp environment more extensive during the 111th century cal BP (). From this date, for the following three centuries, the site saw more extensive and intensive occupation with the successive construction of three large timber platforms at the lake edge and extensive occupation of the dryland, probably including post-build structures (western dryland structure and eastern dryland structure and central dryland structure [338]). Craft activities, including bead manufacture, took place on the wetland edge (area north of Cutting II). An area of intense deposition (*Clark's area*) saw the deliberate accumulation of large quantities of faunal remains, antler headdresses/masks and organic and stone artefacts into an area that was under shallow water, at least seasonally.

As reedswamp gave way to fen carr during the 107th century cal BP (main text Figure 4), the character of occupation at Star Carr changed once more, becoming small-scale and perhaps more episodic. Our evidence consists of a series of small-scale activity areas involving craft activities, such as flintknapping and the production of beads and antler artefacts. Human activity at Star Carr ends in *10505–10330 cal BP (95% probability; end star Carr*; main text Figure 3), probably in *10475–10390 cal BP (68% probability).* It was in use for a period of *735–965 years* (*95% probability*; *use Star Carr;* main text Figure 3), probably over a period of *775–885 years* (*68% probability*).

7b. The lacustrine palaeoenvironmental sequences

7b.1 development of the model

The radiocarbon dates for the Palaeolake flixton lacustrine sequence in Supplementary Table 4 and these were combined with palynological and stratigraphic information from the lake and the lake edge archaeological record (monolith M1) to integrate the archaeological and palaeoenvironmental chronologies. These tie-points are summarised in Supplementary Figure 14. A peak in *Rumex* sp. pollen occurs at 285cm in Core B and 329cm in Core C. A peak in *Filipendula* sp. pollen occurs at 281cm in Core B and 325cm in Core C, and must have occurred before the start of organic deposition in monolith M1. The posterior distribution for *onset organics M1* has therefore been exported from the integrated lake-edge archaeological and palaeoenvironmental model described above and employed as a *terminus ante quem* for this event in the Star Carr cores. A peak in *Salix* sp. pollen also occurs in Cores B and C, at depths of 273cm and 313cm respectively. It also occurs at a depth of 23.62m in monolith M1, where it is bracketed by *OxA-3344* and *OxA-3345*. The posterior distributions for these dates have therefore also been exported from the integrated lake-edge archaeological and palaeoenvironmental model and employed as constraining dates *Salix* peak in the Star Carr cores. The point where *Corylus* sp. pollen reaches 50% of total land pollen, ties Core B (where it occurs at a depth of 212cm) and monolith M1 (where it occurs at a depth of 23.96m) together. The posterior distribution for *hazel 50 TLP* has therefore been exported from the integrated lake-edge archaeological and palaeoenvironmental model and employed as a date for the relevant height in Core B.

The model for the chronology of the climate proxies is exactly defined by the OxCal CQL2 code file star_carr_climate_B_C_to_Vedde_final.oxcal and associated prior distributions.

Supplementary Figure 14 Summary of biostratigraphic tie-points between sediment sequences at Star Carr.

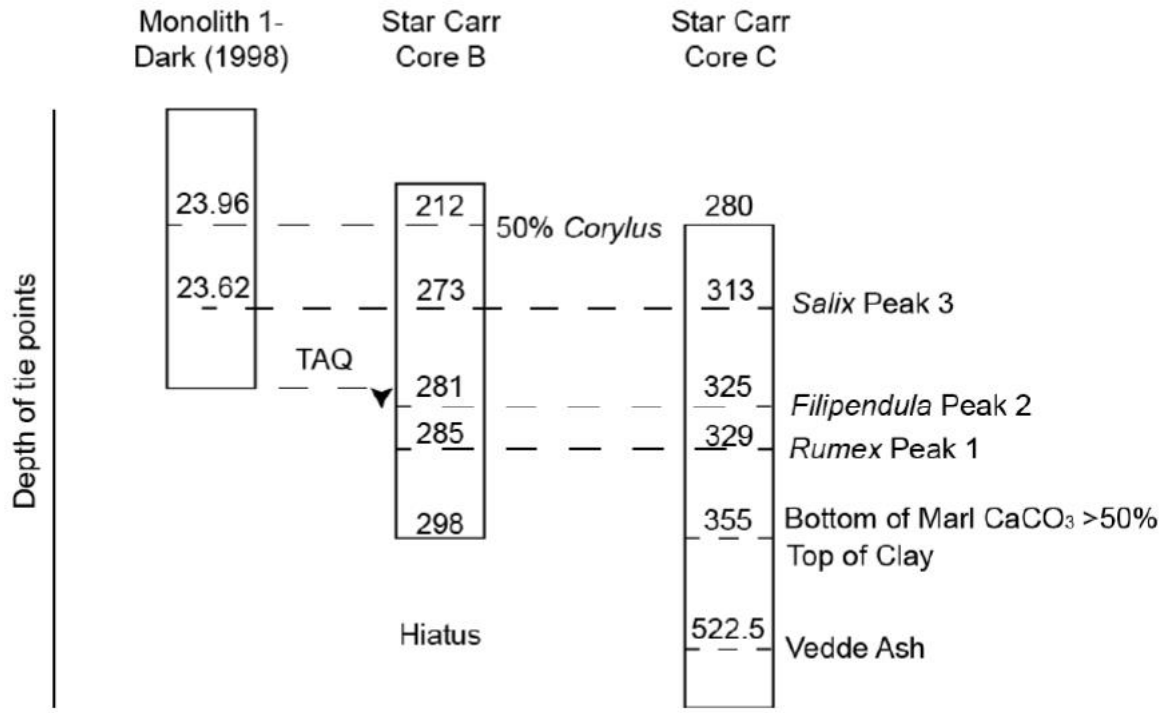

Supplementary Table 4: Radiocarbon results from Star Carr, Core B (quoted $\delta^{13}C$ values were obtained by Isotope Ratio Mass Spectrometry)

Laboratory number	Sample and context description	Radiocarbon age (BP)	$\delta^{13}C$(‰)
OxA-32405	bulk sample of *Betula* sp. fruit (x1) *Carex* sp. seed (x1) and indet twig (x1) seived from a slice of sediment 5cm thick at 21.95–21.91 m OD (145–9cm from surface).	8885±45	−27.0±0.2
OxA-32406	bulk sample of *Populus*-type leaf fragments from a slice of sediment 1cm thick at 21.61–21.60 m OD (179–80cm from surface).	9190±55	−26.2±0.2
OxA-32654	bulk sample of *Betula* sp. leaf fragments seived from a slice of sediment 1cm thick at 21.06–21.05 m OD (234–5cm from surface).	9665±40	−27.9±0.2
OxA-32407	bulk sample of sedge fragments seived from a slice of sediment 1cm thick at 20.69–20.68 m OD (271–2cm from surface).	11870±70	−13.7±0.2
OxA-32655	bulk sample of sedge fragments seived from a slice of sediment 1cm thick at 20.69–20.68 m OD (271–2cm from surface).	11860±50	−12.3±0.2
OxA-32656	bulk sample of sedge fragments seived from a slice of sediment 1cm thick at 20.55–20.54 m OD (285–6cm from surface).	12010±50	−13.6±0.2

Enriched $\delta^{13}C$ values from the samples at and below 271cm in Core B suggest that the samples analysed include components other than the targeted terrestrial plant materials, (methods) which have contributed to the carbon pool and that those components draw carbon from a $\delta^{13}C$ enriched freshwater source. In retrospect, it is likely that this material was included in the small sedge and leaf fragments that were included in many of the samples. As the freshwater source is also depleted in ^{14}C, estimating the proportion of the freshwater-derived organic component in each macrofossil sample is important for the calibration of the radiocarbon ages, as a

calibration using a purely terrestrial calibration curve will produce anomalously early radiocarbon dates.

To estimate the relative contributions of terrestrial-based carbon and freshwater-derived carbon in a given sample, we have developed a basic mixing model using the Bayesian mixing model FRUITS (Food Reconstruction Using Isotopic Transferred Signals[15]. FRUITS is usually employed for the quantitative reconstruction of a consumer's diet by dietary proxies such as stable isotope values (eg $\delta^{13}C$, $\delta^{15}N$, $\delta^{18}S$, etc.) in consumer tissue. However, this sophisticated mixing program may be simplified to estimate for a two-source question about the relative contribution to macrofossil $\delta^{13}C$ from two sources.

The model for the macrofossils is built on the following baseline data and assumptions. The terrestrial baseline is the mean of 22 measured values on a mixture of charred and waterlogged terrestrial plant macrofossils (such as identified pieces of sedge and waterlogged birch fruits) available from the archaeological and palaeoenvironmental deposits at the lake edge. As such, the terrestrial baseline here (−27.2±1.1‰) is not the source carbon that is taken up in photosynthesis, but rather, is the endpoint of expected $\delta^{13}C$ for a fully terrestrial plant. The original freshwater baseline values are from Holocene marl records from Palaeolake Flixton (Supplementary Table 4) which is $CaCO_3$ precipitated from dissolved inorganic carbon (DIC) of the lake waters. These $\delta^{13}C$ values are used as a proxy for the carbon values which fully aquatic plants incorporated via photosynthesis. However, the varying marl $\delta^{13}C$ values are representative of a source, rather than an endpoint similar to that of the terrestrial baseline value.

As the terrestrial endpoint represents the atmospheric carbon value and the fractionation effect contributed by photosynthetic metabolism, the values on the lake-origin marl must be similarly transformed. A fractionation constant of −6.38‰, with a standard deviation of 3.3‰ was calculated from the difference between source carbon values and plant tissue values for four aquatic macrophytes[16; tab. 2]. For each depth, the given freshwater base value from the marl and the fractionation constant of −6.38‰ were combined, the error for each sample being a weighted mean of the respective marl value standard deviation and the standard deviation on the fractionation constant. The adjusted freshwater baseline is an endpoint similar to the terrestrial baseline values (Supplementary Table 5). The FRUITS model assumed an equal (100%) concentration of either terrestrial or freshwater for the proportional calculation. No prior was used to further constrain the calculations.

Supplementary Table 5 provides estimates of the proportional $\delta^{13}C$ contribution of freshwater-based material that may have been incorporated into each of the dated macrofossil samples. Three of the macrofossil samples have $\delta^{13}C$ values which are highly enriched compared to the fully terrestrial baseline used in the FRUITS model (−27.2‰±1.1‰). The FRUITS model

estimates that the freshwater-sourced component in these samples ranges between 63±6% and 70%±7% (Supplementary Table 3).

Supplementary Table 5: The three macrofossil samples from the upper part of core B with $\delta^{13}C$ values suggestive of a component of freshwater-based material, the baseline values used for the FRUITS modelling, and the estimates of the proportion of the sampled carbon deriving from each reservoir.

Lab. Number	Target sample material	$\delta^{13}C$ (‰)	Terrestrial Baseline $\delta^{13}C$ (‰)	Freshwater Baseline (marl) $\delta^{13}C$ (‰)	Adjusted Freshwater Baseline $\delta^{13}C$ (‰)	Terrestrial Proportion (%)	Freshwater Proportion (%)
OxA-32407	Sedge fragments	−13.7±0.2	−27.2±1.1	0.5±0.4	−5.88±1.85	37±6	63±6
OxA-32653	Sedge fragments	−12.3±0.2	−27.2±1.1	0.5±0.4	−5.88±1.85	30±7	70±7
OxA-32656	Sedge fragments	−13.6±0.2	−27.2±1.1	0.47±0.43	−5.91±1.87	37±6	64±6

In order to calibrate these radiocarbon dates from Core B accurately, it is necessary to estimate the freshwater reservoir age of Lake Flixton. Unfortunately, we have no 'perfect pairs' of fully aquatic and fully terrestrial macrofossils at the same depth. The closest approximations that we have are two samples from the upper part of core B at 271-2cm from the surface (OxA-32655, 70±7% freshwater and OxA-32407, 63±6% freshwater), which can be related by a peak in willow pollen to a sample of fully terrestrial plant macrofossils at 23.65–23.655m OD in the M1 profile from the lake edge at Star Carr (6; OxA-3344; 9360±70 BP). The peak of willow pollen in core B occurs at 273cm (1.5cm below the dated samples) and the peak of willow pollen in M1 occurs at 23.62m (3cm above the dated sample).

First we calculate the offset between each pair of values [17, eq. 2 and 3], and then increase this proportionately according to the estimated amount of freshwater-derived carbon in the sample provided by the FRUITS modelling (Supplementary Table 5). The two reservoir estimates produced by this methodology from 271-2cm in core B are not statistically consistent (T′=10.0,

T′(5%)=3.8; ν=1[18]), and so we have taken a weighted mean and increased the error so that both estimated values are included at 2σ. This approach produces estimates for the Freshwater reservoir effect in Lake Flixton of 3743±121 BP.

To calibrate the three reported radiocarbon ages which have enriched $\delta^{13}C$ values, we have constructed a specific mixed-source calibration curve for each of these samples. This mixes the fully terrestrial curve for the northern hemisphere (IntCal1[47]) with the appropriate freshwater reservoir for Lake Flixton in the proportion suggested by the FRUITS model for that particular sample, using the Mix_Curves function of OxCal v4.2[48,]). So, for example, OxA-32656 (Core B upper, 285-6cm) has been calibrated using a calibration curve including a component of 64±6% of the Holocene freshwater reservoir (note that the proportion of any curve is constrained to be 0–100%). The remainder of dated sample would have been in equilibrium with the contemporary atmosphere and have been calibrated using IntCal13[47].

7.b.2 model outputs

Key parameters for changes in climate and vegetation around Star Carr are illustrated in Supplementary Figure 15, with Highest Posterior Density intervals for these parameters provided in Supplementary Table 6. The estimates for the duration of the climate and environmental events around Star Carr are illustrated in Supplementary Figure 15.

Supplementary Figure 15 Probability distributions for changes in climate and vegetation around Star Carr, derived from the model defined exactly in star_carr_climate_B_C_to_Vedde_final.oxcal.

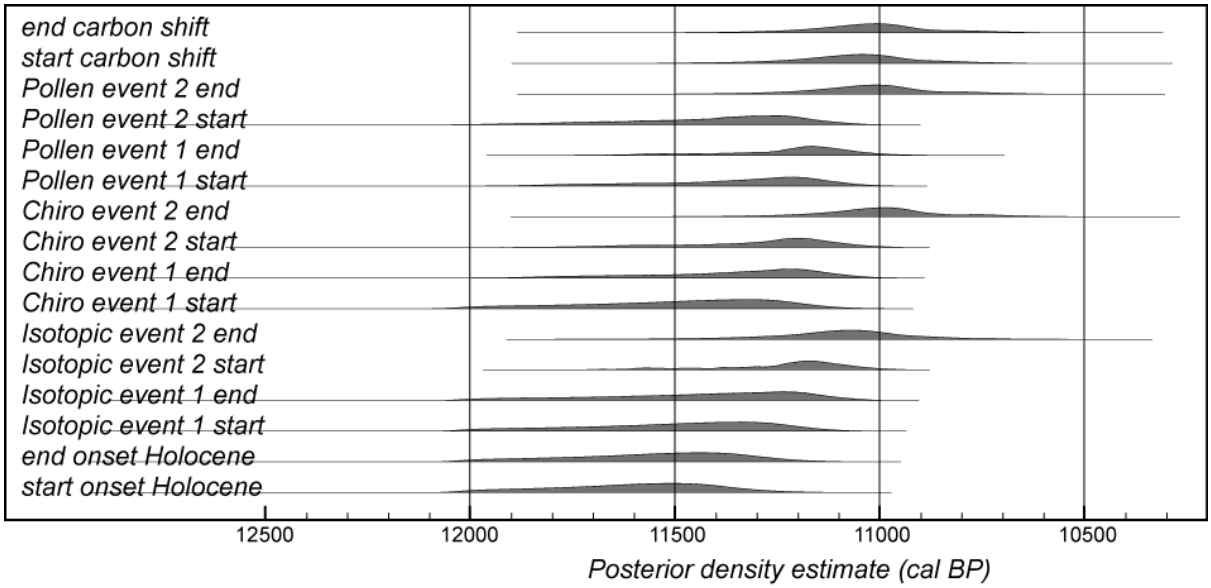

Supplementary Table 6 Highest Posterior Density intervals for changes in climate and vegetation around Star Carr, derived from the model defined exactly in star_carr_climate_B_C_to_Vedde_final.oxcal.

Parameter	**Core & depth**	***Highest Posterior Density interval***	
		95% probability	***68% probability***
start onset Holocene	Core C, 400cm	*12005–11275 cal BP*	*11765–11365 cal BP*
end onset Holocene	Core C, 387cm	*11995–11215 cal BP*	*11725–11290 cal BP*
Isotopic event 1 start	Core C, 371cm	*11975–11140 cal BP*	*11660–11205 cal BP*
Isotopic event 1 end	Core C, 355cm	*11965–11070 cal BP*	*11610–11125 cal BP*
Isotopic event 2 start	Core B, 284.5cm	*11615–10980 cal BP*	*11330–11040 cal BP*
Isotopic event 2 end	Core B, 267.5cm	*11460–10745 cal BP*	*11240–10935 cal BP*
Chiro event 1 start	Core C, 368cm	*11965–11130 cal BP*	*11650–11190 cal BP*
Chiro event 1 end	Core C, 344cm	*11815–11040 cal BP*	*11485–11095 cal BP*
Chiro event 2 start	Core B, 288cm	*11700–11005 cal BP*	*11400–11070 cal BP*
Chiro event 2 end	Core B, 260cm	*11320–10640 cal BP*	*11155–10875 cal BP*
start carbon shift	Core B, 265cm	*11410–10710 cal BP*	*11210–10915 cal BP*
end carbon shift	Core B, 262cm	*11360–10670 cal BP*	*11185–10895 cal BP*
Pollen event 1 start	Core C, 343cm	*11470–11095 cal BP*	*11795–11040 cal BP*
Pollen event 1 end	Core C, 325cm	*11610–10960 cal BP*	*11320–11035 cal BP*
Pollen event 2 start	Core B, 295cm	*11870–11065 cal BP*	*11550–11145 cal BP*
Pollen event 2 end	Core B, 262cm	*11360–10670 cal BP*	*11185–10895 cal BP*

Supplementary Figure 16 Probability distributions for durations of climatic and environmental events around Star Carr, derived from the model defined exactly in star_carr_climate_B_C_to_Vedde_final.oxcal and calculated by Star_Carr_Climate_Summary.oxcal.

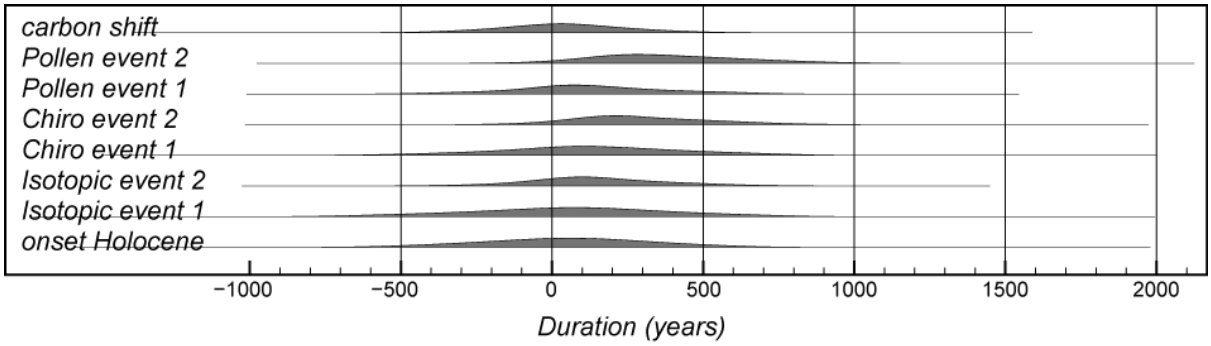

The Bayesian model gives age ranges for a set of defined events taken from the climate and environmental proxies (see main text Figure 4). The Younger Dryas/Holocene transition is clearly recorded most clearly in the abrupt shift at 400cm in $\delta^{18}O$ in core C (Supplementary Figure 16) and dates to *12005–11275 cal BP* (*start onset Holocene*) to *11995–11215 cal BP* (*end onset Holocene; 95% probability*) , most likely *11765–11365 cal BP* to *11725–11290 cal BP* (*68% probability*; Supplementary Table 6). This is followed in the sedimentary record by a shift from minerogenic inwashed sediments deposited in the Younger Dryas (reflecting a cold climate and open vegetation characterised by landscape erosion) to carbonate rich endogenic, lake marls (reflecting warm climates, high productivity and increased vegetation cover). This shift is also seen in the pollen with cold climate assemblages (grasses and shrubs) in the Younger Dryas being replaced by temperate climate vegetation (*Betula, Pinus, Corylus*) during the early Holocene. The chronology of this record would imply that the climatic history recorded in this sequence was in phase with the transition recorded in Greenland, as the GICC05 age (11653 $\pm$ 99 BP (1950), converted from b2k) for the onset of the Holocene matches well with the timing of this transition in Palaeolake Flixton.

8. Abrupt climatic events in the early Holocene

Abrupt climatic events in the Early Holocene, whilst being of sufficient magnitude to potentially disrupt and impact on early societies, may often appear subdued in palaeoenvironment proxy records. For example, the widely discussed 8.2 ka event, in Britain produces a decline in the δ18O values of lacustrine carbonates of 0.8 per mill[19] and a decrease of chironomid-based temperature reconstructions that are within the uncertainties of the technique[20]. Consequently, it is essential for researchers to be confident that oscillations that are observed in the proxy records are truly "climatic events" and not background noise within the signal. In this study we define ACE's on the basis of the following criteria: 1) cooling recorded in both chironomid-based temperature reconstructions and $\delta^{18}O$ values, 2) a centennial-scale duration (Supplementary Figure 15; and main text Figure 4) a response in the local environment to these events through a shift in the vegetation assemblage. While both climate proxies respond to these forcing events the expression and timing of their response differ, as they record different components of the seasonal climate signal.

The first climate event (ACE1 from main text Figure 4) is recorded in the $\delta^{18}O$ signal at *11975-11140 cal BP* (*95% probability; Isotopic depletion 1 start;* Supplementary Table 6) most likely *11660-1105 cal BP (68% probability).* This ends at *11965-11070 cal BP (95% probability; Isotopic event 1 end)* most likely in *11620-11125 cal BP* (*68% probability*), with the $\delta^{18}O$ signal recording a decline of ~2‰. It is also clearly observable as a 1°C decline in CI-T commencing at *11965-11132 cal BP* (*95% probability; Chiro event 1 start;* Supplementary Table S6) most likely at *11655-11190 cal BP* (*68% probability*) and ending at *11815-11040*

cal BP (*95% probability; Chiro event 1 end*) most likely *11485-11095 cal BP* (*68% confidence*).

The second event (ACE2) is clearly expressed in the $\delta^{18}O$ signal (decline by ~1.5‰) commencing at *11615-10980 cal BP (95% probability; Isotopic event 2 start*; Supplementary Table 6*)* most likely *11330-11040 cal BP* (*68% probability*). This event ends at *11460-10745 cal BP* (*95% probability; Isotopic event 2 end*) most likely at *11240-10935 cal BP(68% probability).* The timing of these events as recorded in $\delta^{18}O$ are used to define the timing of abrupt climate events ACE 1 and ACE 2 in the main text (Figure 4). It is also recorded as a cooling of 1 to 1.5ºC in the chironomid-based temperature record commencing at *11695-11005 cal BP (95% probability; Chiro event 2 start)* most likely at *11400-11070 cal BP (68% probability)* and ending at *11320-10640 cal BP (95% probability; Chiro event 2 end)* most likely at *11155-10875 cal BP (68% probability)*. The local environmental response to the climate signal is seen in the pollen profiles for the site (main text Figure 4 and Supplementary Figures 6 and 7) with low tree pollen and increased shrub and herb taxa in pollen events 1 and 2.

Although it is not possibility to absolutely quantify the magnitude of temperature change that a shift in $\delta^{18}O$ represents, it is reasonable to assume that ACE 2 represents a cooling of around 4 degrees. This estimate is based on the suggestion by a number of authors[21,22] that, in freshwater carbonates that form within western Europe, a 1 degree cooling produces an approximate 0.3 decline in the $\delta^{18}O$ of any precipitated carbonates. This is proposed because the two key controls on the $\delta^{18}O$ of freshwater carbonates are; 1) the air temperature control on the $\delta^{18}O$ of rainfall (+0.58 per mill / +1 degree) and 2) the temperature control on isotopic fractionation that occurs during mineralisation (-0.24 to 0.28 per mill / + 1 degree). As these two factors work in opposite directions but the air temperature control on the $\delta^{18}O$ of rainfall is greater his means that whilst a 1 ºC shift in air temperature may propagate a 0.58 to 0.7‰ in the δ18O of an ice-core sequence, the same temperature change would produce only a 0.3‰ shift in the δ18O of a lacustrine carbonate sequence[23]. It is, therefore, likely that the isotopic shifts of ACE1 and 2 represent higher magnitude temperature changes than comparable events in the ice-core records despite being of similar magnitude. Consequently, the decline in $\delta^{18}O$ that is recorded in ACE 2 can be considered to equate to an approximate cooling of the order of 4 degrees and 10 degrees for ACE 1.

As well as abrupt climate events the palaeoenvironmental record also documents longer term changes in local environment, as a response to the establishment of Holocene conditions and the gradual succession of the lake and the local vegetation. This come in the form of macrofossils (Supplementary section 3), total tree pollen (main text Figure 4 and Supplementary Figures 6 and S7) and the stable carbon $\delta^{13}C$ values for the lake sediments (main text Figure 4). The timing of changes in the environment of the site at the lake edge are shown in Figure 4 (and are derived from the lake-edge archaeological and palaeoenvironmental model). The shifts in $\delta^{13}C$ and total tree pollen are also shown in the main text Figure 4. It is clear from these figures that a key transition in the record occurs around the time of a significant shift in the carbon isotope record in the deep lake cores between *11410–10710 cal BP* (*95% probability; start carbon shift*) and *11360–10670 cal BP* (*95% probability; end carbon shift*), most likely between *11210–10915 cal BP* and *11185–10895 cal BP* (*68% probability*), which closely matches the transition into Environmental zone 2 in the lake edge record (main text Figure 4). These environmental transitions have a much greater impact on the activities at Star Carr than the abrupt climate events. After these environmental transitions there is an increase

in platform construction, most likely reflecting the impact of the change to reedswamp and increasing dominance of trees in the landscape.

References for Supplementary

1. Clark J. G. D. *Excavations at Star Carr: an early Mesolithic site at Seamer near Scarborough, Yorkshire* (Camb. Univ. Press, 1954).
2. Schadla-Hall R.T. Recent investigations of the early Mesolithic landscape in the Vale of Pickering, East Yorkshire. *Mesolithic Northwest Europe: recent trends* (eds Zvelebil M. & Blankholm H.) 46-54 (Univ. of Sheff., 1987).
3. Schadla-Hall R. T. The Vale of Pickering in the Early Mesolithic in context. *The Mesolithic in Europe Papers presented at the Third International Symposium, Edinburgh, 1985* (ed Bonsall C.) 218-224 (John Donald, Edinburgh, 1989).
4. Cloutman E. W. & Smith A. G. Palaeoenvironments in the Vale of Pickering Part 3: environmental history at Star Carr. *Proc. Prehist. Soc.* **54,** 37-58 (1988).
5. Day P. Devensian Late-Glacial and early Flandrian environmental history of the Vale of Pickering, Yorkshire, England. *J. Quat. Sci*. **11,** 9–24 (1996).
6. Dark P. Palaeoecological investigations. *Star Carr in context: new archaeological and palaeoecological investigations at the early Mesolithic site of Star Carr, North Yorkshire* (eds Mellars P. & Dark P.)11-120 (McDonald Institute for Archaeological Research, 1998).
7. Palmer A. P. *et al*. The evolution of Palaeolake Flixton and the environmental context of Star Carr, NE. Yorkshire: stratigraphy and sedimentology of the Last Glacial-Interglacial Transition (LGIT) lacustrine sequences. *Proc. Geol. Assoc.* **126,** 50-59 (2015).
8. Cloutman E. W.. Palaeoenvironments in the Vale of Pickering Part I: stratigraphy and palaeogeography of Seamer Carr, Star Carr and Flixton Carr. *Proc. Prehist. Soc.* **54,** 1-19 (1988).
9. Taylor, B. et al. Resolving the Issue of Artefact Deposition at Star Carr. *Proc. Prehist. Soc.* 83, 23–42 (2017).
10. *Star Carr, Volume 2: studies in technology, subsistence and environment*. (eds Milner, N., Conneller, C. & Taylor, B.) (White Rose University Press: York, in press).
11. Langdon P. G., Ruiz Z., Wynne S., Sayer C. D. & Davidson T. A. Ecological influences on larval chironomid communities in shallow lakes: implications for palaeolimnological interpretations. *Fresh. Biol.* **55,** 531-545 (2010).
12. Brooks S. J. & Birks H. J. B. Chironomid-inferred air temperatures from late-glacial and Holocene sites in north-west Europe: progress and problems. *Quat. Sci. Rev.* **20,** 1723-1741 (2001).
13. Medeiros A. S., Gajewski K., Porinchu D. F., Vermaire J. C. & Wolfe B. B. Detecting the influence of secondary environmental gradients on chironomid-inferred palaeotemperature reconstructions in northern North America. *Quat. Sci. Rev.* **124,** 265-274 (2015) .
14. R Core Team *R: A language and environment for statistical computing R Foundation for Statistical Computing* http://wwwR-projectorg/ (Vienna, Austria) (2015).
15. Fernandes R., Millard A. R., Brabec M., Nadeau M. J. & Grootes P. Food reconstruction using isotopic transferred signals (FRUITS): a Bayesian model for diet reconstruction PLoS ONE 9 (2014).
16. Keeley J. E. & Sandquist D. R. Carbon: freshwater plants. Plant Cell Environ. 15, 1021-1035 (1992).
17. Soulet G. Methods and codes for reservoir–atmosphere 14C age offset calculations Quat. Geochron. 29, 97-103 (2015).

18. Ward G. K. & Wilson S. R. Procedures for Comparing and Combining Radiocarbon Age-Determinations – Critique. Archaeometry 20, 19-31 (1978).
19. Marshall J. D., l, J.D., Lang, B., Crowley, S.F., Weedon, G.P., van Calsteren, P., Fisher, E.H., Holme, R., Holmes, J.A., Jones, R.T., Bedford, A., Brooks, S.J., Bloemendal, J., Kiriakoulakis, K. & Ball, J.D., Terrestrial impact of abrupt changes in the North Atlantic thermohaline circulation: early Holocene, UK. *Geology* **35,** 639-642 (2007).
20. Lang B, Brooks, S.J., Bedford, A., Jones, R.T. & Birks, H.J.B. Regional consistency in Lateglacial chironomid-inferred temperatures from five sites in north-west England. *Quat. Sci. Rev.* **29,** 1528-1538 (2010).
21. Andrews J. E. Palaeoclimatic records from stable isotopes in riverine tufas: Synthesis and review. *Earth Sci. Rev.* **75,** 85-104 (2006).
22. Candy, I., Stephens, M., Hancock, J.D.R. & Waghorn, R.S. Palaeoenvironments of ancient human occupation: the application of oxygen and carbon isotopes to the reconstruction of Pleistocene environments. *The Ancient Human Occupation of Britain Project. Developments in Quaternary Science*, (eds Ashton, N., Lewis, S.G. & Stringer, C.) 23-37 (Elsevier, 2011).
23. Candy, I., Abrook, A, Elliot, F, Lincoln, P, Matthews, I & Palmer, A. Oxygen isotopic evidence for high-magnitude, abrupt climatic events during the Lateglacial Interstadial in northwest Europe: Analysis of a lacustrine sequence from the site of Tirinie, Scottish Highlands. *J. Quat. Sci.* **31,** 607-621 (2016).